applied sciences

MDPI

Article

Magnetic Fields Trump Oxygen in Controlling the Death of Erythro-Leukemia Cells

Ying Li [1] and Paul Héroux [2,*]

[1] Plastic and Reconstructive Surgery, McGill University Health Center, Montreal, QC H4A 3J1, Canada; ying.li1@mail.mcgill.ca

[2] Department of Epidemiology, Biostatistics and Occupational Health, McGill University, Montreal, QC H3A 1A2, Canada

* Correspondence: paul.heroux@mcgill.ca; Tel.: +1-514-398-6988

Received: 6 October 2019; Accepted: 3 December 2019; Published: 6 December 2019

Abstract: Expansions in power and telecommunications systems have created a new electromagnetic environment. Here, we compare the death rate of human cancer cells in vitro in the pre-industrial electromagnetic environment of the past ("Zero Field") with that of an electromagnetic environment typical of contemporary human exposures ("Incubator Field"). A cell incubator provides magnetic fields comparable to those in the current human environment. Steel shields divert those same fields away from cell preparations in the "pre-industrial" assays. Large changes in oxygen levels are provided by nitrogen or atmospheric gas over the cell cultures. Human cancer cells are then separated according to three categories: necrotic, early apoptotic, or late apoptotic. The results are compiled for two variables, magnetic field and oxygen, in 16 different situations ("Transitions") likely to occur in the human body under present living conditions. We find that magnetic fields are a more powerful determinant of cell death than oxygen, and induce death by different mechanisms. This has important implications for the reproducibility of in vitro biological experiments focusing on cell survival or metabolism, and for public health. The rate and mechanisms of cell death are critical to many chronic human ailments such as cancer, neurological diseases, and diabetes.

Keywords: electromagnetic field; ELF; cellular phone; necrosis; apoptosis; K562

1. Introduction

Exposure to man-made electromagnetic radiation (EMR) consists of two main parts. First and oldest are extra-low-frequency magnetic fields (ELF MFs, 50/60 Hz) from power systems. Humans are commonly exposed to MFs reaching 1 μT or more in proximity to electrical power [1], but exposure is much smaller when far away from electrical devices and networks.

The second part involves radio-frequency carriers (RF, 3 kHz to 300 GHz) for transmission of analog or digital signals. RF signals carrying digital signals contain substantial ELF MFs, because of their use of data bursts. In the case of the global system for mobiles (GSM), with carriers near 900 and 1750 MHz, ELF components at 8.3, 217, and 1750 Hz [2] are present. A cellular phone user is therefore exposed to ELF MFs emitted by the cell phone antenna, plus the pulsed MFs from the phone's battery, such peak fields rating as high as 95 μT at the head during actual GSM handset use [3]. The range of 0 to 1 μT for ELF MFs chosen for investigation in our work is therefore relevant to both power system and cellular phone exposures [4].

In the results to follow, we compare effects of variations in MFs (0 to 1 μT) to those of variations in oxygen levels. Incubator levels are as high as 18.6%, and, in the human body, 13% in large systemic arteries, falling rapidly along the arterial tree to tissue values of 5 to 0.6%. As much as 82% of oxygen readings in solid tumors are less than 0.33% [5]. Many cells in the body are subjected to oxygen level

variations corresponding to changes in perfusion (as a result of exercise or vasodilatation), or because white blood cells can lodge in different tissues. We have therefore chosen the widest practical range of oxygen variations in our experiments: from the 18.6% present in incubator air ("High O_2") to the 0.4 to 0.7% ("Low O_2") maintained over cultures initially flushed with anoxic medical gas.

Our interest in MF changes stems from our previous observations on oxygen [6] and on MFs where, even using a variable as blunt as karyotype, cancer cells needed more than a month to recover from a 0 to 1 μT transition, and changes as small as 0.01 μT triggered cell adaptations [7].

Within the MF range of 0 to 1 μT, various environmental sources of EMR combine to create human exposures that are highly variable over multiple time scales, best described by the term "fractal instability". The slowest layer of exposure complexity is provided by the user's transient use of a cellular phone or powered device, while the protocols of cellular phone data transmissions contribute faster layers. Digital techniques use sudden transitions to carry signals (bits) because these provide a high signal to noise ratio. Carriers are further manipulated with frame and burst structures, and time and frequency-domain-multiple-access, to increase data carrying capacity. Beam-forming using dipole arrays, proposed for 5G, adds further space segmentation to the previously used time and frequency segmentations. Under the assumption that human physiology needs to adapt to this fractal instability of EMR, it becomes important to evaluate changes in EMR exposures for potential impacts on human health.

In environmental toxicology, the efficacy of an agent in eliciting toxic responses (here, necrosis and apoptosis) is often obtained from the measurement of outcomes within the range of exposures present in the environment. Oxygen is one of the most scrutinized agents in biology, while environmental EMR is a subject of much controversy. Comparing the two agents over their intensity ranges is instructive of their relative physiological influence. We therefore attempted the simulation of the range of MFs (0 to 1 μT) and oxygen levels (High and Low O_2) present in the human body to investigate this question.

2. Materials and Methods

2.1. Cells and Culture Medium

K562 cells from the ATCC were maintained at 5% CO_2, 90% humidity, and overlaid with anoxic gas or conventional atmosphere (21% O_2) as needed. The culture medium was RPMI-1640 with l-glutamine (Sigma 61-030-RM, Millipore Sigma, Oakville, ON, Canada) and 5% fetal bovine serum (Multicell, Wisent, St-Bruno, QC, Canada) without antibiotics, contained in vented T-25s (Sarstedt 83.1810.502, St. Leonard, QC, Canada) or T-12s (Falcon 353018, Thermo Fisher Scientific, Saint-Laurent, QC, Canada). Cells were seeded at 5000/cm^2, and passaged every 6 days.

"High O_2" cultures were placed within a CO_2 incubator with atmospheric gas, while "Low O_2" hypoxic cultures were maintained using large air-tight 4.8 L polycarbonate containers (Lock & Lock, StarFrit, boul. Guimond, St-Bruno, QC, Canada) flushed with 95% medical grade nitrogen and 5% CO_2 [8]. Oxygen levels were measured in the overlying gas (OxyCheck, Kerry Road, Archerfield, Australia) before (0.4%) and after (0.7%) the experiments.

2.2. Magnetic Fields

The "Incubator Field" was meant to represent common environmental conditions, but was so named because it is also typical of laboratory cell culture conditions. From previous surveys, the range of 1 to 5 μT AC included 44% of incubators [9], and 10 to 55 μT DC 76% of incubators [10]. The surrounding environmental ELF MFs are thought to be only weakly attenuated (18 to 33%) by doubled-walled stainless steel enclosures [9]. Our incubator, a Forma 3310 (323 L, Thermo Fisher Scientific, Saint-Laurent, QC, Canada), within which all experiments were performed, had a low average ELF MF (0.4 μT) because of its size.

The two "Incubator Field" test bays, on the middle shelf and along the left side of the incubator, were measured at 1.03 and 1.1 μT AC (EFA-300, Narda, Mississauga, ON, Canada), and 26.4 and 24.8 μT DC (AlphaLab Milligaussmeter, AlaphaLab, Salt Lake City, UT, USA), respectively.

The two "Zero Field" test bays were obtained by surrounding cell cultures in other locations within the same incubator with three concentric metal shields (Figure 1), each 6.3 mm in thickness.

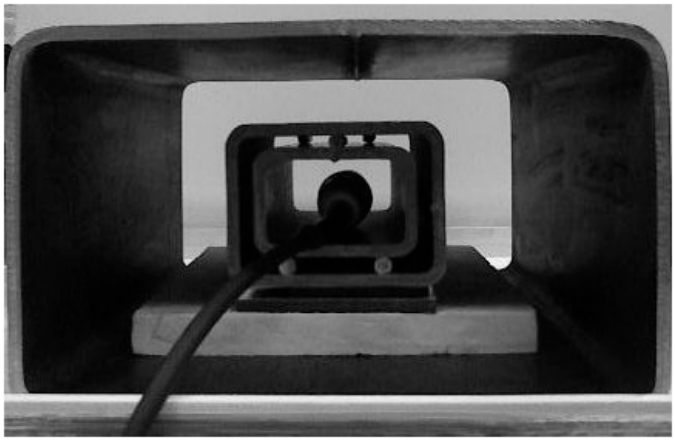

Figure 1. Three concentric steel shields providing a magnetic field attenuation of 144, with the Narda EFA-300's magnetic field probe inserted at the culture position.

A rectangular structural steel beam 5.1 × 7.6 × 20 cm long was inserted inside another beam 7.6 × 10.2 mm of the same length, and both were placed within a third 15.2 × 24.5 × 36 cm long beam. This reduced ELF MFs from the incubator and the environment by a factor of 144, to 3 nT at 60 Hz, slightly below the measurement floor (5 nT at 60 Hz) of our Narda instrument. The static fields in the two "Zero Field" bays were 36 and 38 μT. No MFs, either DC or AC, were electrically applied in any of the tests.

Figure 1 shows the arrangement of steel shields, with the EFA-300's magnetic field probe inserted at the culture position. When needed, boxes for oxygen control (hypoxia) were fitted within the exterior shield, but surrounding the two interior shields.

Figure 2 compares the ELF MF densities measured in the "Zero Field" and "Incubator Field" positions. The "Incubator" MFs are dominated by 60 Hz and 180 Hz components. Harmonics (180 Hz, 300 Hz, etc.) are generated by static power supplies that use semiconductors for power conversion. These nonlinear loads may reside in the incubator itself, or in other devices connected to the electrical network. Signals below 30 Hz are electronic noise from the EFA-300 instrument.

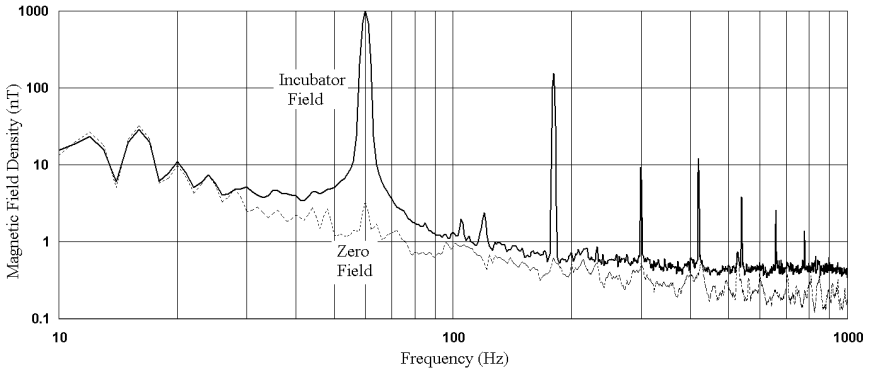

Figure 2. Spectral distribution of magnetic field density at "Incubator Field" and "Zero Field" positions. The 60-Hz component of "Incubator Field" corresponds to 1 μT.

2.3. Cell Culture Measurements

Cell counts, apoptosis, and necrosis readings were obtained by micro-capillary aspiration and miniaturized laser fluorescence detection, performed automatically by a Muse Cell Analyzer cytometer (Millipore Sigma, Oakville, ON, Canada). Total cell count and cell viability were obtained using Millipore assay kit MCH100102, based on the differential permeability of two DNA-binding dyes. Culture media containing K562 cells and the assay kit reagent were added directly to microcentrifuge tubes (VWR 16466-030, VWR International, Ville Mont-Royal, QC, Canada). Five minutes later, the Muse Cell Analyzer delivered counts and viability readings. These readings were used to adjust seeding density at each culture passage.

The Muse Cell Analyzer with Millipore Annexin V & Dead Cell assay kit MCH100105 provided the early apoptosis, late apoptosis, and necrosis readings. K562 cells and the assay kit reagent were added directly to microcentrifuge tubes (VWR 16466-030). Twenty minutes later, the Muse Cell Analyzer delivered readings from evaluation of 1000 cells. The assay relied on the binding of fluorescently labeled Annexin V to phosphatidylserine, which translocates to the outer surface of the cell membrane, exposed in the case of dead and apoptotic cells. Annexin V-Phycoerythrin tagged phosphatidylserine on the external membrane of apoptotic cells. 7-Aminoactinomycin D (7-AAD), because it is excluded from live and healthy cells, and has a strong affinity for DNA, permeated the late-stage apoptotic and dead cells. These determinations allowed the distinction of three cell populations within a culture, as shown in Table 1.

Table 1. Cell Analyzer separation according to necrosis, and early or late apoptosis.

Cell Categories	Annexin V Result	7-AAD Result
Died via necrosis, not by apoptosis	−	+
In early stages of apoptosis	+	−
In late stages, or dead by apoptosis	+	+

Although measurements on effects of EMR have been made previously using similar end-points [11–15], none used environmental level exposures ("Incubator Field") [16], nor, most importantly, pre-industrial fields ("Zero Field") as a reference.

3. Results

3.1. Baseline Experiments

As shown in Table 2, the four environments of the first column differ in MFs (Zero or Incubator) and/or oxygen levels (Low or High). There were only four cell culture bays within a single incubator used throughout the tests. Two bays were "Zero Field", and two bays were "Incubator Field". For each pair of bays, one culture had high oxygen, and the other low oxygen.

To prepare for the Transition results of Table 3, separate cells cultures were maintained under the four baselines (first column of Table 2) for 5 weeks. These conditions were maintained at all times, except for 10 min during the weekly passages (re-seeding at 5000/cm^2) in a sterile hood. The measurements reported in Table 2 were started after this 5-week stabilization.

Table 2. 4 to 6 (*n*) identical experiments for each magnetic field/oxygen condition yield the percentage of Dead K562 cells in baseline cultures. Actual numbers of cells counted are obtained by multiplying the percentages by 1000 × "*n*".

Magnetic Field	Necrosis (%)	Early Apoptosis (%)	Late Apoptosis (%)	Total Death (%)
Oxygen (*n*)	**SD (%)**	**SD (%)**	**SD (%)**	**SD (%)**
Incubator Field	0.45	6.35	7.83	14.63
High O_2 (*6*)	38	50	9.7	19
Incubator Field	0.67	5.77	8.7	15.13
Low O_2 (*6*)	32	45	14	24
Zero Field	0.5	3.83	9.3	13.63
High O_2 (*4*)	35	32	28	20
Zero Field	0.47	3.77	6.27	10.5
Low O_2 (*4*)	32	52	63	55
Average (20)	0.52	4.93	8.03	13.47
	17	23	14	13

Table 3. Triplicate relative necrosis, early apoptosis, and late apoptosis death results relative to baselines ± SD for all Transitions. Assuming normal distributions, 56% of the 36 mean/SD ratios individually reach $p < 0.05$, and 89% $p < 0.13$ against the null hypothesis.

Transferred to / Starting Culture	Incubator Field High O_2	Incubator Field Low O_2	Zero Field High O_2	Zero Field Low O_2	
Incubator Field/High O_2	1	1.3 ± 0.5	2.7 ± 1.3	3.5 ± 1.9	**NECROSIS**
Incubator Field/Low O_2	4.2 ± 2.8	1	4.46 ± 2.2	3.1 ± 1.5	
Zero Field/High O_2	3.9 ± 2.6	4.21 ± 3.1	1	1.62 ± 0.7	
Zero Field/Low O_2	4.1 ± 2.37	3.7 ± 2.1	3.9 ± 1.8	1	

Transferred to / Starting culture	Incubator Field High O_2	Incubator Field Low O_2	Zero Field High O_2	Zero Field Low O_2	
Incubator Field/High O_2	1	0.31 ± 0.12	1.05 ± 0.2	2.6 ± 1.1	**EARLY APOPTOSIS**
Incubator Field/Low O_2	1.2 ± 0.33	1	2.5 ± 0.9	1.5 ± 1.1	
Zero Field/High O_2	1.33 ± 0.5	2.3 ± 1.2	1	0.3 ± 0.19	
Zero Field/Low O_2	1.65 ± 0.82	1.28 ± 0.45	0.8 ± 0.45	1	

Transferred to / Starting culture	Incubator Field High O_2	Incubator Field Low O_2	Zero Field High O_2	Zero Field Low O_2	
Incubator Field/High O_2	1	2.4 ± 1.12	1.1 ± 0.65	2.7 ± 0.89	**LATE APOPTOSIS**
Incubator Field/Low O_2	0.9 ± 0.46	1	1.85 ± 0.81	1.4 ± 0.62	
Zero Field/High O_2	1.06 ± 0.83	2.9 ± 1.21	1	3 ± 1.51	
Zero Field/Low O_2	2.2 ± 0.72	1.02 ± 0.58	0.7 ± 0.53	1	

3.2. Baseline Cell Culture Results

We documented the baseline cell death rates in the four different environments listed in the first column of Table 2. Table 2 was obtained by repeatedly growing cell cultures under the same conditions of MF and oxygen (same test bay) 4 to 6 times (according to "*n*" in Table 2). This procedure is identical to the 5 week stabilization period above, with the difference that at each weekly passage, the number of cells dead from necrosis, early apoptosis, or late apoptosis [17] were counted, and averaged together as presented in Table 2.

Measurements for each of the 4 conditions showed variations (SD in Table 2) over the 4 or 6 repeats, because cultures turned out slightly differently at each harvest. Cultures grown under identical conditions were different because of operational variations: the random seeding process could not be done with perfect control of cell density, the "fresh" culture medium aged over time, and there were small differences in laboratory technique.

Standard deviations (SDs) were different for each variable: necrosis (32–38%), early apoptosis (32–52%), and late apoptosis (9.7–63%). In spite of these variations, in Table 2, the "Average" line at the bottom showed relatively small SDs ranging from 14 to 23% among the four baseline cultures, indicating that death mechanisms do not differ that much between different environmental conditions, but that differences can occasionally be large among individual cultures grown under a nominally identical condition.

In Table 2, Total Death (last column) from either necrosis or apoptosis varied from 10.5 to 15.13%, according to the culture condition, but apoptosis (early or late) was 25 times more frequent, overall, than necrosis. "Zero MF-Low oxygen" showed a 27% lower Total Death (10.5%) than the other baselines. The "Incubator MF-High oxygen" baseline culture showed lower necrosis (0.45%) compared to "Incubator MF-Low oxygen" (0.67%). "Incubator MF-Low oxygen" induced the most necrosis (0.67%). "Zero Field" baselines had a higher late/early apoptosis ratio.

Accurate measurements of environmental perturbations (changes in MF, oxygen, or both) could only be obtained if a test was simultaneously run as an unperturbed control to compensate for the re-seeding instability documented in the baseline cultures of Table 2. This was obtained as follows.

A pipette drawing from a well mixed cell culture flask was used to seed with the same number of drops four identical culture flasks. The four flasks were deposited in the four different environments shown in the first column of Table 2. One of the four, the original environment of the culture, served as an unperturbed control. A week after these passages, the four cultures were assessed with the Muse for necrosis, early, and late apoptosis. This procedure was performed three times in succession for each baseline condition, and results are shown in Table 3. This maximized the accuracy of in vitro determinations, since for each of the 12 (or 3×4) Transition measurements, an undisturbed control was always available that used the same source culture, the same medium, simultaneous manipulations under the hood, and were grown in the same incubator.

3.3. Transition Cell Culture Results

Our main series of results measured the impact on cell death of changes in MFs or oxygen level, "single Transitions", or changes in both MF and oxygen, "double Transitions", compared to similar readings on cells dying from passage into an unchanged environment, growing at the same time. Tests were done three times in succession for each of the four baseline cultures of Table 2. The Transitions were intended to simulate, in an incubator microcosm, the full range of variations occurring in a human body within the current modern environment.

In Table 3, the shaded "1" diagonal cells represent relative readings from cells passaged to fresh medium, but with unchanged oxygen and/or MF conditions (the controls).

Results larger than 1 in Table 3 represent the increased number of cells dying as a result of adaptations to MFs and/or oxygen. Results smaller than 1 indicate that the new environment improved cell survival, compared to baseline. Overall, Transitions are more likely to cause cell death than simple passage, as only 5 out of 36 Transitions in Table 3 show ratios smaller than 1. Repeatability of our measurements on aliquots was 4%.

The results of Table 3 are further displayed (differently) in Figure 3 and Table 4.

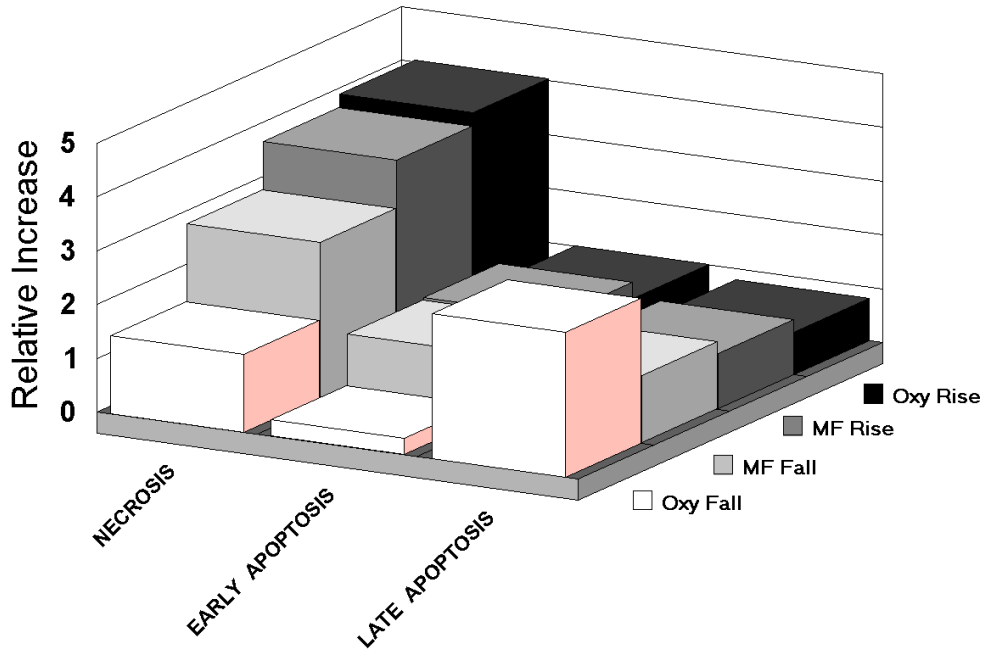

Figure 3. Relative amounts of necrosis, early, and late apoptosis associated with oxygen falls/rises and magnetic field (MF) falls/rises.

Table 4. Cell death analysis for all Transitions, relative to baselines. Oxygen "rise" is L% to H%. "Fall" is H% to L%. MF "rise" is Zero to Incubator Field. "Fall" is Incubator to Zero Field. "H%", "L%", "Zero", and "Incu" refer to unchanged conditions. Total damage = necrosis + late apoptosis + early apoptosis. "Δ" is the ratio of maximum to minimum on a line.

Oxygen	**Rise**	**Fall**	**Rise**	**Rise**	**H%**	**Rise**	**L%**	**Fall**	**L%**	**H%**	**Fall**	**Fall**	**Δ**
MF	**Fall**	**Rise**	**Incu**	**Rise**	**Rise**	**Zero**	**Rise**	**Fall**	**Fall**	**Fall**	**Zero**	**Incu**	
Necrosis	4.46	4.21	4.2	4.1	3.9	3.9	3.7	3.5	3.1	2.7	1.62	1.3	3.4
Late Apoptosis	1.85	2.9	0.9	2.2	1.06	0.7	1.02	2.7	1.4	1.85	3	2.4	4.3
Early Apoptosis	2.5	2.3	1.2	1.65	1.33	0.8	1.28	2.6	1.5	0.3	0.3	0.31	8.7
All Apoptosis	4.35	5.2	2.1	3.85	2.39	1.5	2.3	5.3	2.9	2.15	3.3	2.71	3.5
Late/Early Apoptosis	0.74	1.26	0.75	1.33	0.80	0.88	0.80	1.04	0.93	6.17	10.00	7.74	13.5
Total Damage	8.81	9.41	6.3	7.95	6.29	5.4	6	8.8	6	4.85	4.92	4.01	2.4
Necrosis/Apoptosis	1.03	0.81	2	1.06	1.63	2.6	1.61	0.66	1.07	1.26	0.49	0.48	5.4

Figure 3 graphs the relative amounts of necrosis, early, and late apoptosis associated with oxygen falls, oxygen rises, MF falls, and MF rises, irrespective of the level of the other agent (oxygen or MF). Oxygen rise, MF rise, and MF fall have modest differences between them, while oxygen fall has a very different signature.

Table 4, derived from Table 3, summarizes the twelve possible Transitions in relation to cell death mechanisms. The lines of Table 4 inform on the magnitude of the three cell death mechanisms, on the ability of apoptosis to reach its conclusion (late or early), as well as on the relative importance of necrosis and apoptosis, which is relevant to inflammation.

3.4. Necrosis

All single Transitions, rise or fall, oxygen or MF, enhanced necrotic cell death (values in the first line of Table 4 larger than 1). But oxygen rise (hyperoxic) Transitions were more powerful (4.2, 3.9) than hypoxic ones (1.62, 1.3). MF rises at (3.9, 3.7) and MF falls (3.1, 2.7) rested between these extremes. MF changes only ((2.7 + 3.1 + 3.9 + 3.7)/4 = 3.35) were overall more powerful than oxygen changes only ((1.3 + 4.2 + 1.62 + 3.9)/4 = 2.76) in inducing necrosis.

Table 4 also shows that overall, double Transitions (MF plus oxygen changes) generated more cell death than single MFs or oxygen Transitions ((4.46 + 4.21 + 4.1 + 3.5)/4)/(3.35 + 2.76)/2) = 1.33).

The largest amplification of necrosis (4.46) occurred in the double Transition of Incubator to Zero MF (MF fall), and Low to High oxygen (oxygen rise).

3.5. Early Apoptosis

Transitions either enhanced or attenuated cell death, in contrast to necrosis, where only enhancements were observed.

Single hypoxic Transitions clearly reduced early apoptosis (0.3, 0.31). Single Transition MF rises (1.33, 1.28) weakly enhanced early apoptosis, while MF falls (1.5 at Low oxygen and 0.3 at High oxygen) were obviously strongly influenced by the oxic level.

Here, contrary to necrosis, single oxygen ((1.2 + 0.8 + 0.3 + 0.31)/4 = 0.65) and MF Transitions ((1.33 + 1.5 + 1.28 + 0.3)/4 = 1.1) worked, on average, in opposite directions (attenuation vs. enhancement).

Double Transitions were clearly effective ((2.5 + 2.3 + 1.65 + 2.60)/4 = 2.26), while singles were mild attenuations ((0.65 + 1.1)/2 = 0.88). The strongest effect was for hypoxic MF fall (2.6).

3.6. Late Apoptosis

Many single Transition tendencies were reversed here from what is found in necrosis. Late apoptosis was enhanced by hypoxic Transitions (3, 2.4), and relatively indifferent to hyperoxic Transitions (0.9, 0.7), while MFs rises were much less damaging (1.06, 1.02) than MF falls (3, 2.4).

Similar to necrosis at 4.07, double Transitions (rising diagonals of Table 3) produced 2.41 times more late apoptosis enhancement, higher than single Transitions in oxygen (0.9, 0.7, 3, 2.4), or especially MF (1.06, 1.02, 1.4, 1.85).

In a hyperoxic Transition, addition of a MF change (1.85, 2.2) produced more damage than when the MF was unchanged (0.9, 0.7). The strongest effect was for hypoxia at Zero MF (3).

3.7. Late to Early Apoptosis Ratio

The late/early apoptosis ratio rose to high values (10, 7.74) in hypoxic Transitions without MF change, which means that the large majority of cells then rushed to complete apoptosis.

3.8. Necrosis vs. Apoptosis

Whether cells die by necrosis or apoptosis is important with respect to inflammation. From Table 4, hyperoxia increased the necrosis/apoptosis ratio for both stable Incubator (2) and Zero (2.6) MFs. But a simultaneous change in MF superposed to these hyperoxic rises eliminated the effect on the necrosis/apoptosis ratio (2 > 1.03, 2.6 > 1.06): MF rises and falls attenuated hyperoxic necrosis (reperfusion injury in surgery).

Hypoxia decreased the necrosis/apoptosis ratio under both Incubator (0.48) and Zero (0.49) MFs. But superposition of a simultaneous change in MF attenuated these favorable shifts (0.48 > 0.66, 0.49 > 0.81). MF rises and falls suppressed hyperoxic necrosis, and enhanced hypoxic necrosis. The largest necrosis over apoptosis enhancement observed in Table 4 was 2.6, for hyperoxia under Zero Field.

4. Discussion

Necrosis is the most acute form of cell death, the unregulated disposition of cell components. The loss of cell membrane integrity and release of internal cell elements into the extracellular space trigger the immune system, as invading leukocytes and phagocytes produce an inflammatory response. Damaging substances aimed at microbial control are released by leukocytes, which creates collateral damage to surrounding tissues.

In contrast, apoptosis is programmed cell death that recycles cellular components. Apoptosis occurs naturally in humans, for example in shaping developing organisms. Excessive apoptosis shrinks organs, whereas an insufficient amount may, in some cases, result in cancer. It is triggered by the extrinsic pathway (FAS), or by the intrinsic pathway, notably by increase in cell stress due to the level of reactive oxygen species (ROS) in mitochondria. It avoids the immune response of necrosis by a sequence of steps: caspase activation, blebbing, cell shrinkage, enzymatic hydrolysis, chromatin condensation, chromosomal DNA fragmentation, mRNA decay, and apoptotic body formation. Inflammation is avoided by absorption of the apobodies by surrounding cells.

Apoptosis typically cannot stop once it has begun, but can be found in various stages in cells under stress that have insufficient ATP resources to execute later apoptotic steps. The rate and mechanisms of cell death in cultures can forecast the destiny of human tissues, particularly when considering chronic diseases.

Turning to our results comparing oxygen and MF, Figure 3 isolates the character of the MF from that of oxygen by ignoring the alternate variable in the compilation. An important contrast between oxygen rise and fall, with reasonably similar characteristics for MF rise and fall, suggests different basic lethality mechanisms.

In oxygen fall (hypoxia), apoptosis dominated necrosis, opposite to what was observed in the three other cases. This difference between oxygen rise and oxygen fall is not unexpected, considering that human cells have a natural resistance to hypoxia, mediated by hypoxia-inducible factors as reviewed in [18], which upregulate several genes to promote survival in low-oxygen conditions.

The similarity in patterns for MF rise and fall, observed here, is a particularity we have reported before in relation to MFs and karyotype measurements [7]. The MF rise, as it impairs proton movement in ATP Synthase, increases the mitochondrial membrane potential ($\Delta\Phi m$). If the potential is restored by compensating cellular controls [19], suppression of the field then causes a decrease in the potential. The slight asymmetry between MF rise and fall data (Figure 3), may represent an actual adaptation of the oxidative phosphorylation (OXPHOS) process to the presence of the MFs, and may ultimately lead to uncovering a biological marker for MF exposure.

Deviations of less than 3% from the optimal mitochondrial membrane potential ($\Delta\Phi m$) of 139 mV result in reduced ATP, and increased ROS [20,21]. Such a narrow optimal value is not infrequent in physiology, another prominent example in mitochondria being non-heme iron concentration [22]. As OXPHOS is affected by variable EMF levels from the environment over time, mitochondria work more frequently outside their optimal range.

Yet, because both consumption of oxygen and MFs are known to induce ROS in reviews [23,24], the similarity between oxygen rise, MF rise, and MF fall is expected: MFs and oxygen share some common ground in ROS induction.

Because 31 out of 36 Transitions are deleterious (>1 in Table 3), it is also clear that changes in both variables induce physiological stress, by the way of increasing requirements on physiological adaptations. Various Transitions altered necrosis differently (Δ = 3.4 in Table 4), but the most Transition-sensitive variables were early apoptosis (Δ = 8.7) and the late/early apoptosis ratio (Δ = 13.5). Since checkpoints in the apoptotic process include verification of ATP supply [25], demands on ATP by physiological adaptations retarded the apoptotic process, reducing the late/early apoptosis ratio. This delay in apoptosis, coupled with ROS stress, diverted some of the cells undergoing apoptosis under MF Transitions to necrosis [26].

Our previous work [7] as well as that of others [27,28] has shown that EMR perturbs the movement of free electrons and protons along the OXPHOS chain of enzymes (Complex I to V). Complex V, otherwise known as ATP synthase, is itself a serial system, dependant on the tunneling of protons through a channel containing a string of 10 molecules of water [29]. EMR reduces the transparency of ATP synthase channels, increasing the mitochondrial membrane potential ($\Delta\Phi m$). This increased $\Delta\Phi m$ pushes cells towards a cancer phenotype [30–32], resulting in documented changes in growth rate, morphology, survival rate and chromosome numbers in cancer cells [7].

Many of our observations support the inhibition of OXPHOS and ATP synthesis by MFs.

1. "Zero" MF conditions (facilitated ATP synthesis) should favor a higher late/early apoptosis ratio. Table 2 shows that this is true for baseline cultures at both High (2.43 > 1.23) and even Low (1.66 > 1.51) oxygen.
2. The hypoxic Zero MF Transition of Table 4 had the highest late/early apoptosis ratio (10) of any Transition. When Incubator fields were applied to the same hypoxic Transition, the late/early apoptosis ratio fell by 23%.
3. Although hypoxia was effective at inducing apoptosis (5.2, 5.3, 3.3, 2.71 in Table 4), to induce it quickly, as shown by a high late/early ratio, the MF must be unchanging (10, 7.74). This rapid apoptosis was almost completely inhibited (1.26, 1.04 in Table 4) if a MF change was superposed, constraining ATP resources.
4. Transitions columns in Table 4 are ordered from left to right by decreasing necrosis rating. In the left half of the Table (high necrosis), all MFs are changing, except in two cases, which correspond to hyperoxic rises. Larger shifts in cellular environments, as simultaneous oxygen and MF changes, placed a heavier adaptive load on cells, requiring 5'-adenosine monophosphate-activated protein kinase alpha (AMPK to manage more adjustments [33]. These requirements slowed apoptosis, and increased necrosis (left side of Table 4).
5. Table 3 shows that that the rush to late apoptosis of the hypoxic Transitions with no MF change (2.4, 3 in Table 3) attenuated necrosis (0.48, 0.49 in Table 4) by simple apoptosis to necrosis competition. This indicates that MF variations switch cell death from apoptosis to (inflammatory) necrosis. But under hyperoxic "Zero" MF, the hyperoxia actually attenuated apoptosis (necrosis/apoptosis = 2.6), which means that hyperoxia, through ROS, was quickly toxic to the apoptotic pathway [34], shifting cells towards necrosis.

Mitochondrial perturbations, and changes in the mechanisms of cell death (necrosis vs. apoptosis) are considered relevant or causative for chronic human diseases such as diabetes [33,35,36], heart disease [37–39], and diseases of post-mitotic tissues such as Parkinson's [40,41], Alzheimer's [42–44], multiple sclerosis, amyotrophic lateral sclerosis [45], autism [46], and psychiatric disease [47]. Tissues with high metabolic rates such as the brain [48,49], physiological systems with an already high ROS load [50] such as the islets of Langerhans [51,52], and processes of sperm formation [53] would be particularly vulnerable.

It is not unexpected that environmental EMR exposures would impact many human diseases [54], because undermining ATP supply and the stability of its regulation connects directly to ROS. When the foundations of a building are de-stabilized, many rooms can feel the tremor. A better perspective on MF effects in our environment will emerge as more diverse cell models are investigated.

5. Conclusions

Use of a pre-industrial electromagnetic environment as a reference, and oxygen over a wide range for comparison, reveals the potential sanitary influence of ELF radiation.

ELF from power systems [6,7] or from telecommunications signals [27,28] may have important effects on public health [29].

The ranges chosen here for MFs and oxygen may underplay the relative importance of MFs, as there are many regulators of oxygen in the human body such as breathing rate, vasodilatation, hemoglobin binding, and diffusion. Technological EMR has no physiological regulators, that would need to be developed over evolutionary periods, but elicits only toxic reactions.

MF changes were more potent than oxygen changes in determining the number of cells lost to necrosis and apoptosis. Although hyperoxias with no MF change produced the largest increases in necrosis to apoptosis ratio (2 and 2.6 in Table 4), Total Damage average for single MF Transitions (5.79) was higher than Total Damage average for single oxygen Transitions (5.16). Single MF Transitions, either rises (1.62) or falls (1.17), steered dying cells towards necrosis, rather than apoptosis.

How cells die in human tissues is important, because death by apoptosis recycles cell material, while death by necrosis creates inflammation, a critical component of many chronic diseases that have increased in the last century. Our past results [7] made MF exposures relevant to cancer; our new results on necrosis to apoptosis make them relevant to the chronic evolution of tissues in human populations.

Most of the effects reported can be explained by inhibition of the OXPHOS pathway hosted within the mitochondria of living cells, the consequent rise in ROS generation, and by metabolic dysregulation.

OXPHOS has been the foundation of all life on Earth for at least 2 billion years, while, in stark contrast, human exposures to MF and wireless radiation result from recent technological choices.

The ATP energy produced by the OXPHOS reaction is so critical to biological organisms that it is believed to be the driving force of evolution, with an ominous warning from an evolutionary biologist, "tamper with this reaction at your peril" [55].

Non-natural EMR signals have evolved tremendously in quantity and complexity over the last century. The need for perpetual cellular adaptation to randomly changing environmental fields consumes ATP and oxygen, and disturbs the anterograde and retrograde links between cell nucleus and mitochondria [56,57].

Analog modulations may have posed fewer and smaller risks than the new digital modulations widely introduced recently by communication systems. Most engineering efforts to expand wireless data rates result in an enrichment of the artificial EMR environment that increases biological risks. Biological systems are sensitive not only to the carrier, but to its transitions as well. Such non-natural fields cannot easily avoid biological impacts at either the low frequency or high frequency end of the spectrum [58], or with any modulation scheme.

Author Contributions: Conceptualization, methodology, data analysis, and writing, P.H. Validation and project administration, Y.L.

Funding: This research received no external funding.

Acknowledgments: To Louis Slesin for reviewing the article.

Conflicts of Interest: The authors declare no conflict of interest.

References

1. Héroux, P. A Dosimeter for Assessment of Exposures to ELF Fields. *Bioelectromagnetics* **1991**, *12*, 241–257. [CrossRef] [PubMed]
2. Van der Vorst, A.; Rosen, A.; Kotsuka, Y. *RF/Microwave Interaction with Biological Tissues*; Wiley-Interscience: Hoboken, NJ, USA, 2006; p. 119.
3. Perentos, N.; Iskra, S.; McKenzie, R.J.; Cosic, I. Simulation of pulsed ELF magnetic fields generated by GSM mobile phone handsets for human electromagnetic bioeffects research. *Australas. Phys. Eng. Sci.* **2008**, *31*, 235–242. [CrossRef] [PubMed]
4. Blackman, C. Cell phone radiation: Evidence from ELF and RF studies supporting more inclusive risk identification and assessment. *Pathophysiology* **2009**, *16*, 205–216. [CrossRef] [PubMed]
5. Höckel, M.; Vaupel, P. Tumor hypoxia: Definitions and current clinical, biologic, and molecular aspects. *J. Nat. Cancer Inst.* **2001**, *93*, 266–276. [CrossRef] [PubMed]
6. Li, Y.; Héroux, P.; Kyrychenko, I. Metabolic restriction of cancer cells in vitro causes karyotype contraction—An indicator of cancer promotion? *Tumor Biol.* **2012**, *33*, 195–205. [CrossRef] [PubMed]
7. Li, Y.; Héroux, P. Extra-Low-Frequency Magnetic Fields alter Cancer Cells through Metabolic Restriction. *Electromagn. Biol. Med.* **2014**, *33*, 264–275. [CrossRef]
8. Wright, W.E.; Shay, J.W. Inexpensive low-oxygen incubators. *Nat. Protoc.* **2006**, *1*, 2088–2090. [CrossRef]
9. Su, D.; Héroux, P. Survey of Extra-Low Frequency and Very-Low Frequency Magnetic Fields in Cell Culture Incubators. *arXiv* **2012**. Available online: http://arxiv.org/abs/1211.2458 (accessed on 18 April 2019).

10. Portelli, L.A.; Schomay, T.E.; Barnes, F.S. Inhomogeneous Background Magnetic Field in Biological Incubators is a Potential Confounder for Experimental Variability and Reproducibility. *Bioelectromagnetics* **2013**, *34*, 337–348. [CrossRef]
11. Lantow, M.; Viergutz, T.; Weiss, D.G.; Simkó, M. Comparative Study of Cell Cycle Kinetics and Induction of Apoptosis or Necrosis after Exposure of Human Mono Mac 6 Cells to Radiofrequency Radiation. *Radiat. Res.* **2006**, *166*, 539–543. [CrossRef]
12. Kaszuba-Zwoinska, J.; Wojcik, K.; Bereta, M.; Ziomber, A.; Pierzchalski, P.; Rokita, E.; Marcinkiewicz, J.; Zaraska, W.; Thor, P. Pulsating electromagnetic field stimulation prevents cell death of puromycin treated u937 cell line. *J. Physiol. Pharmacol.* **2010**, *61*, 201–205. [PubMed]
13. Emre, M.; Cetiner, S.; Zencir, S.; Unlukurt, I.; Kahraman, I.; Topcu, Z. Oxidative Stress and Apoptosis in Relation to Exposure to Magnetic Field. *Cell Biochem. Biophys.* **2011**, *59*, 71–77. [CrossRef] [PubMed]
14. Juszczak, K.; Kaszuba-Zwoinska, J.; Thor, P.J. Pulsating electromagnetic field stimulation of urothelial cells induces apoptosis and diminishes necrosis: New insight to magnetic therapy in urology. *J. Physiol. Pharmacol.* **2012**, *63*, 397–401. [PubMed]
15. Filipovic, N.; Djukic, T.; Radovic, M.; Cvetkovic, D.; Curcic, M.; Markovic, S.; Peulic, A.; Jeremic, B. Electromagnetic field investigation on different cancer cell lines. *Cancer Cell Int.* **2014**, *14*, 84. Available online: http://www.cancerci.com/content/14/1/84 (accessed on 18 April 2019). [CrossRef]
16. Wang, H.; Zhang, X. Magnetic fields and reactive oxygen species. *Int. J. Mol. Sci.* **2017**, *18*, 2175. [CrossRef]
17. Nikoletopoulou, V.; Markaki, M.; Palikaras, K.; Tavernarakis, N. Crosstalk between apoptosis, necrosis and autophagy. *Biochim. Biophys. Acta* **2013**, *1833*, 3448–3459. [CrossRef]
18. Palazon, A.; Goldrath, A.W.; Nizet, V.; Johnson, R.S. HIF Transcription Factors, Inflammation, and Immunity. *Immunity* **2014**, *41*, 518–528. [CrossRef]
19. Sepehrimanesh, M.; Kazemipour, N.; Saeb, M.; Nazifi, S.; Davis, D.L. Proteomic analysis of continuous 900-MHz radiofrequency electromagnetic field exposure in testicular tissue: A rat model of human cell phone exposure. *Environ. Sci. Pollut. Res.* **2017**, *24*, 13666–13673. [CrossRef]
20. Bagkos, G.; Koufopoulos, K.; Piperi, C. A new model for mitochondrial membrane potential production and storage. *Med. Hypotheses* **2014**, *83*, 175–181. [CrossRef]
21. Bagkos, G.; Koufopoulos, K.; Piperi, C. Mitochondrial emitted electromagnetic signals mediate retrograde signaling. *Med. Hypotheses* **2015**, *85*, 810–818. [CrossRef]
22. Walter, P.B.; Knutson, M.D.; Paler-Martinez, A.; Lee, S.; Xu, Y.; Viteri, F.E.; Ames, B.N. Iron deficiency and iron excess damage mitochondria and mitochondrial DNA in rats. *Proc. Natl. Acad. Sci. USA* **2002**, *99*, 2264–2269. [CrossRef] [PubMed]
23. Yakymenko, I.; Tsybulin, O.; Sidorik, E.; Henshel, D.; Kyrylenko, O.; Kyrylenko, S. Oxidative mechanisms of biological activity of low-intensity radiofrequency radiation. *Electromagn. Biol. Med.* **2016**, *35*, 186–202. [CrossRef] [PubMed]
24. Kivrac, E.F.; Yurt, K.K.; Kaplan, A.A.; Alkan, I.; Gamze, A. Effects of electromagnetic fields exposure on the antioxidant defense system. *J. Microsc. Ultrastruct.* **2017**, *5*, 167–176. [CrossRef] [PubMed]
25. Eguchi, Y.; Shimizu, S.; Tsujimoto, Y. Intracellular ATP Levels Determine Cell Death Fate by Apoptosis or Necrosis. *Cancer Res.* **1997**, *57*, 1835–1840. [PubMed]
26. Elmore, S. Apoptosis: A Review of Programmed Cell Death. *Toxicol. Pathol.* **2007**, *35*, 495–516. [CrossRef]
27. Sanders, A.P.; Joines, W.T.; Allis, J.W. Effects of Continuous-Wave, Pulsed, and Sinusoidal-Amplitude-Modulated Microwaves on Brain Energy Metabolism. *Bioelectromagnetics* **1985**, *6*, 89–97. [CrossRef]
28. Sanders, A.P.; Schaefer, D.J.; Joines, W.T. Microwave Effects on Energy Metabolism of Rat Brain. *Bioelectromagnetics* **1980**, *1*, 171–181. [CrossRef]
29. BioInitiative Working Group. A Rationale for Biologically-based Exposure Standards for Low-Intensity Electromagnetic Radiation 2012. Available online: Bioinitiative.org (accessed on 18 April 2019).
30. Houston, M.A.; Augenlicht, L.H.; Heerdt, B.G. Intrinsic Mitochondrial Membrane Potential and Associated Tumor Phenotype are Independent of MUC1 Over-Expression. *PLoS ONE* **2011**, *6*, e25207. [CrossRef]
31. Forrest, M.D. Why cancer cells have a more hyperpolarised mitochondrial membrane potential and emergent prospects for therapy. *bioRxiv* **2015**, 025197. [CrossRef]

32. Solaini, G.; Sgarbi, G.; Baracca, A. Oxidative phosphorylation in cancer cells. *Biochim. Biophys. Acta* **2011**, *1807*, 534–542. [CrossRef]
33. Cai, Y.; Martens, G.A.; Hinke, S.A.; Heimberg, H.; Pipeleers, D.; Van de Casteele, M. Increased oxygen radical formation and mitochondrial dysfunction mediate beta cell apoptosis under conditions of AMP-activated protein kinase stimulation. *Free Radic. Biol. Med.* **2007**, *42*, 64–78. [CrossRef] [PubMed]
34. Baigi, M.G.; Brault, L.; Néguesque, A.; Beley, M.; El Hilali, R.; Gaüzère, F.; Bagrel, D. Apoptosis/necrosis switch in two different cancer cell lines: Influence of benzoquinone- and hydrogen peroxide-induced oxidative stress intensity, and glutathione. *Toxicol. In Vitro* **2008**, *22*, 1547–1554. [CrossRef] [PubMed]
35. Nishikawa, T.; Araki, E. Impact of Mitochondrial ROS Production in the Pathogenesis of Diabetes Mellitus and its Complications. *Antioxid. Redox Signal.* **2007**, *9*, 343–353. [CrossRef] [PubMed]
36. Fernyhough, P.; Roy Chowdhury, S.K.; Schmidt, R.E. Mitochondrial stress and the pathogenesis of diabetic neuropathy. *Expert Rev. Endocrinol. Metab.* **2010**, *5*, 39–49. [CrossRef] [PubMed]
37. Ren, J.; Pulakat, L.; Whaley-Connell, A.; Sowers, J.R. Mitochondrial biogenesis in the metabolic syndrome and cardiovascular disease. *J. Mol. Med.* **2010**, *88*, 993–1001. [CrossRef] [PubMed]
38. Rocha, M.; Apostolova, N.; Hernandez-Mijares, A.; Herance, R.; Victor, V.M. Oxidative stress and endothelial dysfunction in cardiovascular disease: Mitochondria-targeted therapeutics. *Curr. Med. Chem.* **2010**, *17*, 3827–3841. [CrossRef] [PubMed]
39. Camara, A.K.S.; Bienengraeber, M.; Stowe, D.F. Mitochondrial approaches to protect against cardiac ischemia and reperfusion injury. *Front. Physiol.* **2011**, *2*, 13. [CrossRef]
40. Kones, R. Parkinson's disease: Mitochondrial molecular pathology, inflammation, statins, and therapeutic neuroprotective nutrition. *Nutr. Clin. Pract.* **2010**, *25*, 371–389. [CrossRef]
41. Subramaniam, S.R.; Chesselet, M.-F. Mitochondrial dysfunction and oxidative stress in Parkinson's disease. *Prog. Neurobiol.* **2013**, *106–107*, 17–32. [CrossRef]
42. Ferreira, I.L.; Resende, R.; Ferreiro, E.; Rego, A.C.; Pereira, C.F. Multiple defects in energy metabolism in Alzheimer's disease. *Curr. Drug Targets* **2010**, *11*, 1193–1206. [CrossRef]
43. Sas, K.; Pardutz, A.; Toldi, J.; Vecsei, L. Dementia, stroke and migraine–some common pathological mechanisms. *J. Neurol. Sci.* **2010**, *299*, 55–65. [CrossRef] [PubMed]
44. Moreira, P.L. Mitochondrial dysfunction is a trigger of Alzheimer's disease pathophysiology. *Biochim. Biophys. Acta* **2010**, *1802*, 2–10. [CrossRef] [PubMed]
45. Kawamata, H.; Manfredi, G. Mitochondrial dysfunction and intracellular calcium dysregulation in ALS. *Mech. Ageing Dev.* **2010**, *131*, 517–526. [CrossRef] [PubMed]
46. Haas, R.H. Autism and mitochondrial disease. *Dev. Disabil. Res. Rev.* **2010**, *16*, 144–153. [CrossRef] [PubMed]
47. Scaglia, F. The role of mitochondrial dysfunction in psychiatric disease. *Dev. Disabil. Res. Rev.* **2010**, *16*, 136–143. [CrossRef] [PubMed]
48. Exner, N.; Lutz, A.K.; Haass, C.; Winklhofe, K.F. Mitochondrial dysfunction in Parkinson's disease: Molecular mechanisms and pathophysiological consequences. *EMBO J.* **2012**, *31*, 3038–3062. [CrossRef] [PubMed]
49. Ravera, S.; Panfoli, I. Role of myelin sheath energy metabolism in neurodegenerative diseases. *Neural Regen. Res.* **2015**, *10*, 1570–1571. [CrossRef]
50. Harman, D. Aging: A theory based on free radical and radiation chemistry. *J. Gerontol.* **1956**, *11*, 298–300. [CrossRef]
51. Besse-Patin, A.; Estall, J.L. An Intimate Relationship between ROS and Insulin Signalling: Implications for Antioxidant Treatment of Fatty Liver Disease. *Int. J. Cell Biol.* **2014**, *2014*, 519153. [CrossRef]
52. Wang, X.; Roper, M.G. Measurement of DCF fluorescence as a measure of reactive oxygen species in murine islets of Langerhans. *Anal. Methods* **2014**, *6*, 3019–3024. [CrossRef]
53. Meinhardt, A.; Wilhelm, B.; Seitz, J. Expression of mitochondrial marker proteins during spermatogenesis. *Hum. Reprod. Update* **1999**, *5*, 108–119. [CrossRef] [PubMed]
54. Jornayvaz, F.R.; Shulman, G.I. Regulation of mitochondrial biogenesis. *Essays Biochem.* **2010**, *47*, 69–84. [PubMed]
55. Lane, N. *The Vital Question. Energy, Evolution, and the Origins of Complex Life*; WW Norton & Co: New York, NY, USA; London, UK, 2015.
56. Wolff, J.N.; Ladoukakis, E.D.; Enríquez, J.A.; Dowling, D.K. Mitonuclear interactions: Evolutionary consequences over multiple biological scales. *Philos. Trans. R. Soc. Lond. B Biol. Sci.* **2014**, *369*, 20130443. [CrossRef] [PubMed]

57. Lionaki, E.; Gkikas, I.; Tavernarakis, N. Differential Protein Distribution between the Nucleus and Mitochondria: Implications in Aging. *Front. Genet.* **2016**, *7*, 162. [CrossRef]
58. Winkler, J.R.; Di Bilio, A.J.; Farrow, N.A.; Richards, J.H.; Gray, H.B. Electron tunneling in biological molecules. *Pure Appl. Chem.* **1999**, *71*, 1753–1764. [CrossRef]